

# A Genetically Encoded Optical Probe of Membrane Voltage

## Neurotechnique

Micah S. Siegel<sup>1\*</sup> and Ehud Y. Isacoff<sup>2†</sup>

<sup>1</sup>University of California

Department of Molecular and Cell Biology  
Berkeley, California 94720

<sup>2</sup>California Institute of Technology  
Computation and Neural Systems  
Pasadena, California 91125

### Summary

Measuring electrical activity in large numbers of cells with high spatial and temporal resolution is a fundamental problem for the study of neural development and information processing. To address this problem, we have constructed a novel, genetically encoded probe that can be used to measure transmembrane voltage in single cells. We fused a modified green fluorescent protein (GFP) into a voltage-sensitive K<sup>+</sup> channel so that voltage-dependent rearrangements in the K<sup>+</sup> channel would induce changes in the fluorescence of GFP. The probe has a maximal fractional fluorescence change of 5.1%, making it comparable to some of the best organic voltage-sensitive dyes. Moreover, the fluorescent signal is expanded in time in a way that makes the signal 30-fold easier to detect. A voltage sensor encoded into DNA has the advantage that it may be introduced into an organism noninvasively and targeted to specific developmental stages, brain regions, cell types, and subcellular compartments.

### Introduction

Fluorescent indicator dyes have revolutionized our understanding of cellular physiology by providing continuous measurements in single cells and cell populations. Presently, these dyes must be synthesized chemically and introduced as hydrolyzable esters or by microinjection (Cohen and Leshner, 1986; Tsien, 1989; Gross and Loew, 1989). Delivering indicator dyes to specific cell populations could be a significant advantage for many experiments, but this has proven to be a difficult problem. In the absence of such localization, optical measurements in neural tissue usually cannot distinguish whether a signal originates from electrical activity in neurons or glia, nor which types of neurons are involved. One general approach to this problem is to encode protein-based sensors into DNA. This permits the sensor to be placed under the control of cell-specific promoters and to be introduced in vivo or in vitro using gene transfer techniques.

A protein-based optical sensor must have some means of emitting light. Our approach was to exploit the green fluorescent protein (GFP) cloned from the jellyfish *Aequorea victoria* (Prasher et al., 1992). GFP is a small protein (238 amino acids). Its chromophore is generated autocatalytically (Heim et al., 1994), and the protein is

stable and functional in many cell types. The crystal structure of GFP has been solved by X-ray diffraction (Ormo et al., 1996; Yang et al., 1996), and mutations have been found that alter its spectral properties (Heim et al., 1994), providing some guidance as to how GFP might be modified for new applications. Several recent studies have used GFP to mark gene expression and to trace individual proteins in a wide variety of organisms (Chalfie et al., 1994; Amsterdam et al., 1995; Marshall et al., 1995).

This paper describes a novel GFP-based sensor that we have designed to measure fast membrane potential changes in single cells and in populations of cells. The naturally occurring GFP, a soluble cytoplasmic protein, is not sensitive to the voltage across the plasma membrane. Therefore, we fused GFP to the voltage-activated Shaker K<sup>+</sup> channel (Tempel et al., 1987; Baumann et al., 1988; Kamb et al., 1988). Our idea was that the voltage-dependent structural rearrangements in the channel could be transmitted to GFP, resulting in a measurable change in its spectral properties.

The Shaker–GFP fusion gene that we constructed reports changes in membrane potential by a change in its fluorescence emission. This fluorescence response is amplified in time over the electrical event, drastically increasing the optical signal power per event. Taken together, the properties of genetic encoding and temporal amplification allow the sensor to be delivered to selected cells in which action potentials may be detected with standard imaging equipment.

### Results

#### Fusion Constructs of the Shaker K<sup>+</sup> Channel and GFP

Our goal was to construct a GFP–Shaker fusion protein in which Shaker retains normal conformational rearrangements, the fluorescence of GFP is correlated with these rearrangements, and the protein does not interfere with the physiology of the cells in which it is expressed. We were concerned that Shaker–GFP proteins could disrupt the physiology of the cells in which they were expressed by introducing an extra ionic current. Therefore, the point mutation *W434F* was engineered into the pore region of Shaker. This mutation prevents ion conduction but preserves the channel's gating rearrangements in response to voltage changes (Perozo et al., 1993).

Since the core of the Shaker channel, including the N-terminal assembly domain and the transmembrane segments, is highly conserved (Stuhmer et al., 1989; Drewe et al., 1992; Li et al., 1992; Shen et al., 1993) and therefore probably intolerant to large insertions, we fused GFP in-frame at a site just after the sixth transmembrane segment (S6; Figure 1). The crystal structure of GFP indicates that its C-terminus is disordered from amino acids 230–238 (Ormo et al., 1996; Yang et al., 1996). Since several of these amino acids can be removed without disrupting GFP fluorescence (Dopf and Horiagon, 1996), we deleted amino acids 233–238 (*GFPΔC*).

<sup>†</sup> To whom correspondence should be addressed.

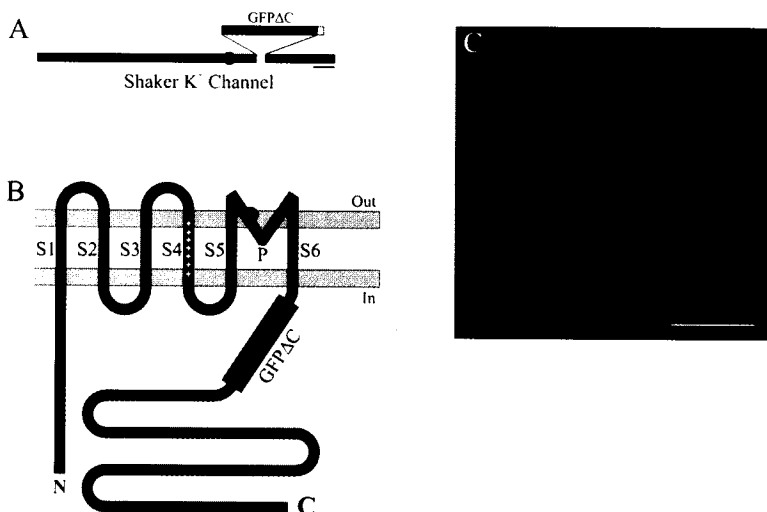


**Figure 1.** FlaSh Is a Fusion Between Shaker K<sup>+</sup> Channel and Modified Green Fluorescent Protein

(A) GFPΔC (green) was inserted in-frame into the Shaker K<sup>+</sup> channel (black). A point mutation W434F (red circle) was made in the pore of the channel to eliminate ionic current through the sensor.

(B) Putative orientation of the FlaSh protein in the cell membrane (gray). The fourth transmembrane segment S4 is positively charged. Note that GFPΔC is intracellular and FlaSh is targeted to the cell membrane.

(C) Xenopus oocytes injected 14 days earlier with cRNA encoding FlaSh (right) show bright membrane fluorescence compared to uninjected oocytes (left), using confocal microscopy.

(A) Scaled according to protein length; scale bar, 50 amino acids; (B) not to scale, (C) scale bar, 500 μm.

with the idea that the structured, fluorescent core of GFP could be tied directly to the moveable parts of the channel (Figure 1).

Xenopus laevis oocytes injected with cRNA transcribed from Shaker-W434F/GFPΔC@S6 (henceforth called FlaSh, for fluorescent Shaker) showed green membrane fluorescence (Figure 1C), indicating that GFP was targeted appropriately. As expected, the W434F mutation abolished ionic current through the sensor. Voltage steps from a holding potential of -80 mV evoked only "on" and "off" gating currents (Figure 2A). Integrating the gating current gives the total charge (Q) moved during the voltage step. The time course of this gating charge movement reveals a fast component in response to small voltage steps and a slow component in response to larger voltage steps. The slow off currents following large depolarizations had the properties described earlier for the wild-type channel, in which inactivation by the N-terminus retards the return of the gating charge (Bezanilla et al., 1991). We concluded that FlaSh retains the normal, Shaker-like gating rearrangements in response to changes in membrane potential.

Voltage-clamp fluorimetry revealed that, remarkably, FlaSh changes its emission intensity in response to voltage steps. Depolarizing steps that moved the slow component of the gating charge and immobilized the off gating charge evoked a decrease in fluorescence from FlaSh (Figure 2A). A maximum fluorescence decrease of  $5.1\% \pm 0.7\%$  ( $n = 7$ ) was observed in response to steps that moved all of the gating charge. Small depolarizing voltage steps, which evoked only the gating charge component that was minor and fast, produced no fluorescence change. The relation of the steady-state fluorescence change to voltage was sigmoidal and correlated closely with the steady-state gating charge-to-voltage relation (Figure 2B). This correlation indicates that, in FlaSh, the fluorescence emission of GFP is coupled to the voltage-dependent rearrangements of the Shaker channel.

The FlaSh protein was very stable, as judged by gating current and fluorescent measurements. Expression did not decline over a period of 2 weeks in Xenopus oocytes. Moreover, no bleaching was visible after >5 min of mea-

surement with nearly continuous broad-band (425–475 nm) excitation. In addition, FlaSh continued to respond to voltage when we increased the temperature from 22°C to 37°C. The rates of both the onset and recovery of the fluorescence change were increased by  $2.0 \pm 0.3$  ( $n = 3$ )-fold at the higher temperature.

#### Kinetics of FlaSh

Although the fluorescence of FlaSh follows the voltage dependence of Shaker activation, the kinetics of the on and off fluorescence changes ( $F_{on}$  and  $F_{off}$ ) were slower than the movement of the gating charge ( $Q_{on}$  and  $Q_{off}$ ; compare F and Q in Figure 2A). At steps to 0 mV,  $Q_{on}$  was ~30-fold faster ( $p < 0.0001$ ) than  $F_{on}$  ( $\tau_{[F_{on}]} = 2.8 \pm 0.4$  ms,  $\tau_{[Q_{on}]} = 85 \pm 10$  ms;  $n = 5$ ). The slower kinetics of the fluorescence change indicate that rearrangement in the voltage sensor of Shaker may trigger but does not directly cause the change in GFP fluorescence.

The fluorescence response of FlaSh cannot be a direct consequence of N-type inactivation because  $F_{on}$  and  $F_{off}$  were slower than the onset and recovery of N-type inactivation. As shown earlier (Bezanilla et al., 1991), the onset of gating charge immobilization, and thus N-type inactivation, closely followed  $Q_{on}$  (Figure 3,  $I_g$ ), which was more than an order of magnitude faster than  $F_{on}$ . Moreover, the immobilized  $Q_{off}$  at -80 mV, following large depolarizations, returned approximately twice as fast ( $p < 0.001$ ) as  $F_{off}$  ( $\tau_{[Q_{off}]} = 72 \pm 7$  ms,  $\tau_{[F_{off}]} = 160 \pm 12$  ms;  $n = 7$ ).

The delay in the fluorescence change may arise from a time-dependent event in GFP, or a slow rearrangement in Shaker. The fluorescence change lacks intrinsic voltage sensitivity, whatever its mechanism, since the time constants of both  $F_{on}$  and  $F_{off}$  saturate at voltages outside of the voltage range of activation (Figure 2C).

#### Stereotypical Fluorescence Output from FlaSh Expands Brief Membrane Transients

To determine whether FlaSh could respond to short-lasting electrical activity, we explored its fluorescence kinetics in response to brief voltage pulses. These voltage transients moved a fraction of the total gating charge, and steps of 3 ms and longer evoked long,

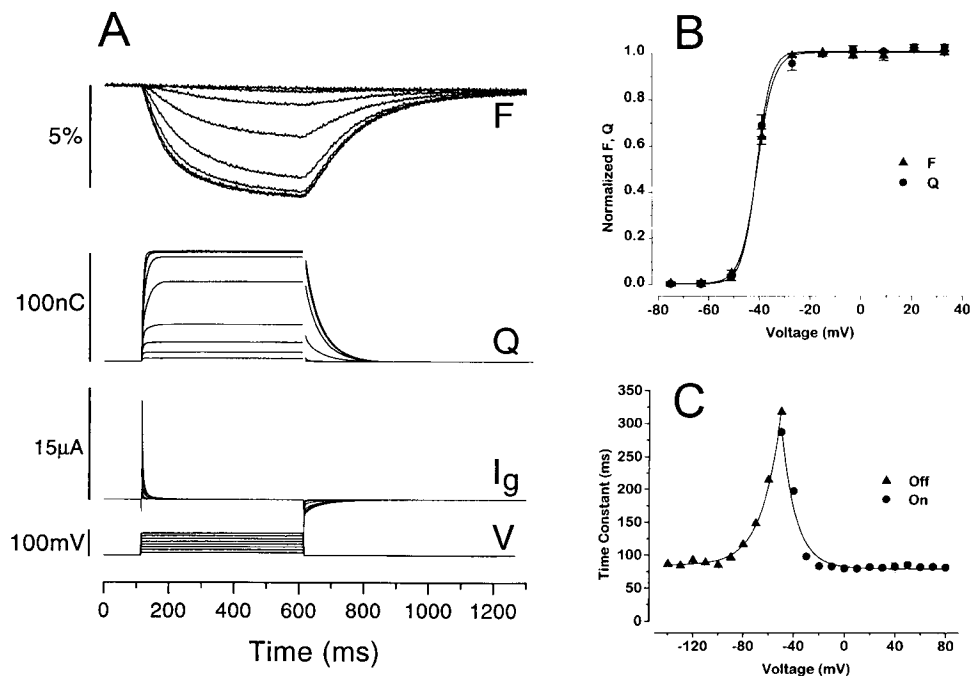


Figure 2. Transmembrane Potential Modulates Fluorescence Output in FlaSh

(A) Simultaneous two-electrode voltage-clamp recording and photometry show current and fluorescence changes in response to voltage steps (V) between  $-60$  mV and  $10$  mV, in  $10$  mV increments. Holding potential was  $-80$  mV. FlaSh exhibits on and off gating currents ( $I_g$ ) but no ionic current. Integrating the gating current gives the total gating charge (Q) moved during the pulse. FlaSh fluorescence (F) decreases reversibly in response to membrane depolarizations. Traces are the average of 20 sweeps. Fluorescence scale,  $5\% \Delta F/F$ .

(B) FlaSh fluorescence is correlated to Shaker activation gating. The voltage dependence of the normalized steady-state gating charge displacement (Q) overlaps with the normalized steady-state fluorescence change (F). Both relations were fit by a single Boltzmann equation (solid lines). Values are mean  $\pm$  SEM from five oocytes.

(C) The kinetics of the fluorescence change are independent of voltage at extreme potentials. The time constant of the decrease in fluorescence during depolarizing steps (On) is shown for  $500$  ms steps from a holding potential of  $-80$  mV to the indicated potential. The time constant of the recovery of fluorescence (Off) is shown for  $1$  s repolarizations to the indicated potential following a  $500$  ms step potential to  $40$  mV. The values were obtained from mono-exponential fits, which accounted well for the on and off fluorescence changes. Both relations are approximated by single exponential fits (solid lines).

stereotypical fluorescent responses (Figure 3). While the magnitude of the fluorescence change was related to the duration of the step, its kinetics of onset and recovery were constant. The entire collection of fluorescent responses was well fit by a double-exponential with time constants of  $23$  ms for  $F_{on}$  and  $105$  ms for  $F_{off}$ . These kinetics are, respectively, 4-fold and 1.5-fold faster than those of the fluorescence changes evoked by long steps.

This stereotyped fluorescence response was clearly visible in single-sweep recordings (Figure 4). Subsequent events that occurred during the time course of the fluorescence change summated with the original response. The unitary responses were visible in the summated response when the trains of electrical events were at frequencies of  $20$  Hz or less. Trains at  $100$  Hz produced a fused response in which the individual events could not be distinguished by eye (but see Discussion).

#### FlaSh Behaves Like a Linear Filter during Spike Trains

For a short train of identical brief pulses, the integral of the fluorescence response was constant at frequencies of  $20$  Hz and lower (Figure 4H) but declined at higher

frequencies. The decline occurred as the peak response approached the maximal fluorescence change, i.e., as the sensor population became saturated. In the low frequency range, a linear filter model with the kinetics of the unitary response based on the stereotypical shape of the FlaSh fluorescence change (Figure 3) accounted well for the shape of the fluorescence response to a pulse train (Figures 4F and 4G). Given the acceleration of FlaSh kinetics when temperature is increased from  $22^\circ\text{C}$  to  $37^\circ\text{C}$ , the maximal firing rate over which FlaSh will be linear may be twice the frequency cutoff of the cooler temperature.

#### Discussion

We have constructed a gene fusion of GFP and the Shaker  $K^+$  channel that changes fluorescence emission in response to changes in membrane potential. The FlaSh protein encoded by this gene makes a stable, bleach-resistant optical voltage sensor with voltage dependence, kinetic properties, and a fractional fluorescence change that should make it useful for the study of fast and slow electrical signaling.

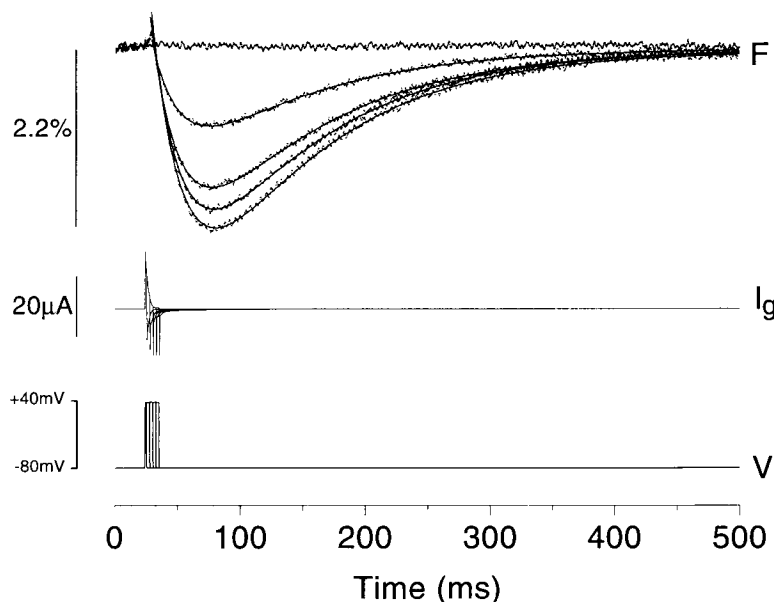


**Figure 3. Brief Depolarizations Evoke Stereotypical Fluorescence Responses**

The fluorescence response of FlaSh following short pulses from  $-80$  mV to  $40$  mV (V) followed a characteristic trajectory that was well fit by a sum of two exponentials with time constants of  $23$  and  $105$  ms (F, solid lines). All but the shortest pulse evoked a delayed fluorescence decrease. All of the voltage pulses evoked gating current ( $I_g$ ). As pulse duration increased, an increasing fraction of the off gating charge returned with very slow kinetics, due to gating charge immobilization by N-type inactivation. Pulses were  $1.25$ ,  $3.75$ ,  $6.25$ ,  $8.75$ , and  $11.25$  ms in duration. Traces are averages of  $25$  sweeps.

### Physiological Impact on Target Cell

To prevent FlaSh from altering the physiology of cells in which it is expressed, we made a point mutation in the Shaker pore that prevents ion conduction. While this works well in oocytes, expression of FlaSh in other cells may introduce the difficulty of FlaSh subunits coassembling with compatible subunits of the same subfamily of channels (Christie et al., 1990; Isacoff et al., 1990; McCormack et al., 1990; Ruppersberg et al., 1990; Covarrubias et al., 1991) and altering the properties of native channels. This may be avoided by linking cDNAs in such a way that the subunits of the channel are covalently attached (Isacoff et al., 1990). While we have not tested FlaSh in mammalian cells, we expect it to work just as well, given the high levels of expression of both Shaker and GFP in a variety of mammalian cell lines.

### Rearrangement Underlying the Change in FlaSh Fluorescence

What causes the fluorescent response of FlaSh? The fluorescence output clearly depends on Shaker activation. However, neither activation nor N-type inactivation can be directly responsible for inducing the fluorescence change, because these processes occur with a much faster time course. Since channel opening normally precedes N-type inactivation (Zagotta et al., 1990), this gating step is also likely to be too fast to directly cause the fluorescence change.

This leaves slower gating rearrangements of the channel, such as those underlying C-type inactivation (Timpe et al., 1988; Hoshi et al., 1990). Indeed, the kinetics of the fluorescence change were consistent with that of C-type inactivation in their voltage dependence (Figure 2C). As with the onset of C-type inactivation (Hoshi et al., 1991), the rate of  $F_{on}$  did not change with steps to voltages more positive than  $-30$  mV; and as with the recovery of C-type inactivation in physiological solution

(Levy and Deutsch, 1996), the rate of  $F_{off}$  varied little at voltages more negative than  $-90$  mV. Interestingly, depolarizations as short as  $3$  ms evoked fluorescent changes with a  $\tau_{(F_{on})}$  of  $23$  ms, indicating that the conformational change responsible for the fluorescence change was triggered by the voltage transient but continued to build up long after the transient was over. This could be explained by the fact that N-type inactivation prevents the channel from deactivating (by immobilizing the gating charge) and thus extends the time over which C-type inactivation can take place to beyond the end of the depolarization (Baukrowitz and Yellen, 1995).

Taken together, these results indicate that the characteristic fluorescence response of FlaSh is initiated by the gating charge movement that accompanies channel activation or by N-type inactivation, but that the mechanism, and therefore the time course, is independent of these processes. Instead, the fluorescence change of FlaSh could be due to C-type inactivation or to another rearrangement in Shaker. Alternatively, the fluorescence change could be due to a slow rearrangement within GFP or to a slow change in the interaction between two or more GFPs in the four subunit channel complex. With regard to this last possibility, oligomerization of GFP does appear to affect its spectral properties (Ward et al., 1982).

Whatever the direct cause of its fluorescence change, four functional states seem to account for the general behavior of FlaSh. Membrane depolarization rapidly pumps the sensor population from a bright resting state ( $R^*$ ) into a bright activated state ( $A^*$ ), from which it slowly decays into a dim activated state ( $A$ ). Repolarization deactivates the sensor from the dim activated state ( $A$ ) into a dim resting state ( $R$ ), from which it slowly returns to the resting bright state ( $R^*$ ). The rate-limiting fluorescent response profile reflects this voltage-independent redistribution of the population of sensors following the voltage-dependent gating events:

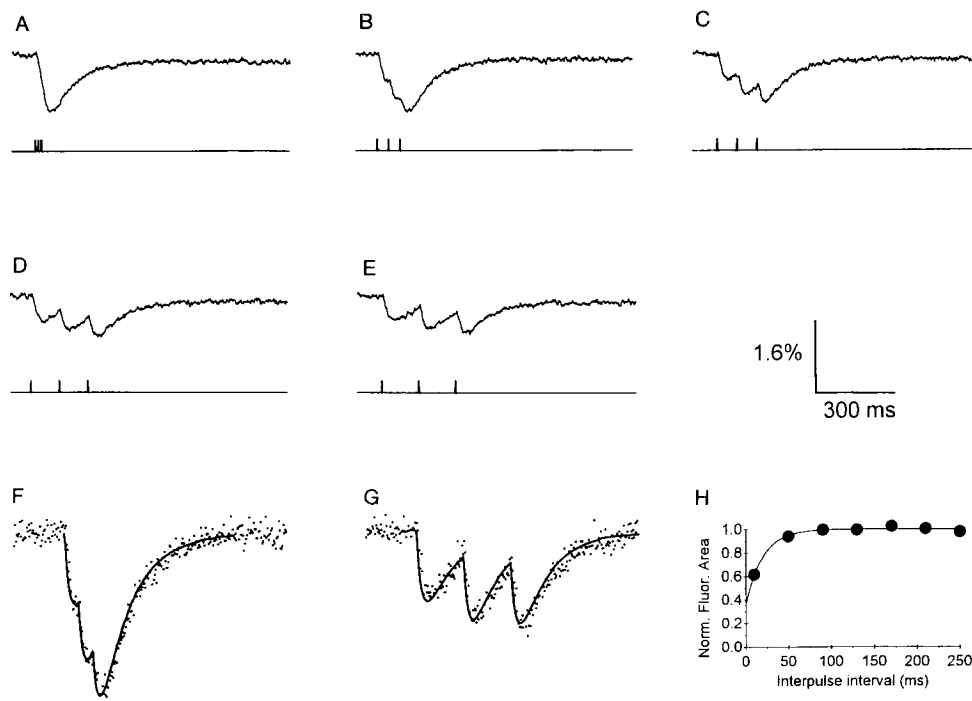


Figure 4. FlaSh Response to Brief Pulses Can Be Detected in Single Sweeps

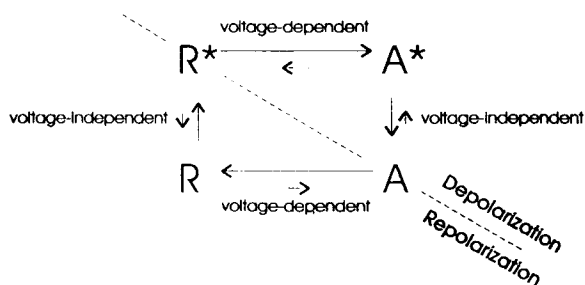
Bursts of short pulses evoked summing responses.

(A–G) Pulses of 4 ms duration from  $-80$  mV to  $40$  mV evoked submaximal fluorescence decreases that summated during a train.

(F–G) The shape of the fluorescence response (noisy trace) could be accounted for by a linear sum of a fit to the stereotypical fluorescence change (solid lines) with  $\tau_{\text{off}} = 23$  ms and  $\tau_{\text{on}} = 105$  ms and a constant impulse size.

(H) The area under the fluorescence response evoked by three pulse trains is linear over a wide range of inter-pulse intervals, indicating a linear summation of responses. The area diverges from linearity at the shortest interval, where the amplitude of the summated response is largest.

Traces in (A) through (G) are single sweeps.



#### How Will FlaSh Report on Neural Activity?

FlaSh is not a typical fluorescent voltage probe. Traditional "fast" voltage-sensitive dyes have been designed to respond quickly and linearly to membrane potential (Cohen and Leshner, 1986; Gross and Loew, 1989; Gonzalez and Tsien, 1997). By contrast, FlaSh provides a different solution to the underlying problem of detecting fast voltage transients: FlaSh gives long, stereotypical fluorescence pulses in response to brief voltage spikes.

The dynamic range of FlaSh is approximately  $-50$  to  $-30$  mV, for depolarizations that are long enough to allow the Shaker channel population to equilibrate. Short depolarizations that do not allow the gating to reach steady-state produce smaller responses at any given voltage. Thus, depolarizations just a few milliseconds in duration that are as large as an action potential ( $\sim 40$

mV) activate only a fraction of the sensor population and evoke submaximal responses. Whether the depolarizations are long or short, FlaSh responds mainly to depolarizations that are above the typical threshold for action potential firing of  $-45$  mV.

#### FlaSh Behavior during Spike Trains

Because brief voltage pulses produce long-lasting, submaximal responses, trains of such pulses—with interpulse intervals shorter than the 500 ms fluorescence recovery time—produced summated responses that were linearly related to the number and frequency of the pulses, making FlaSh into a spike averager (Figure 4). This provides an illustration of how FlaSh, located in excitable neuronal cell bodies and axons, is likely to report on repetitive action potentials firing, since these are also invariant in amplitude and duration. The idea that FlaSh can detect action potentials with a 1 ms duration at  $37^\circ\text{C}$  is based on the fact that single pulses of 3 ms duration activate enough sensors to produce sizable changes in fluorescence at  $22^\circ\text{C}$ , and the kinetics of Shaker activation have a  $Q_{10}$  of  $>3$  (Nobile et al., 1997). In contrast to its characteristic response to action potential depolarizations, FlaSh responds to slower depolarizations—those that more closely resemble dendritic excitatory postsynaptic potentials—with a fluorescence that follows the amplitude and duration of the

depolarization. These two forms of detection are very useful, because neural information is encoded in action potential timing and frequency, as well as in synaptic potential amplitude and duration.

#### Advantages of FlaSh for Detecting Individual Action Potentials

The dynamics of FlaSh provide significant advantages for detecting individual electrical events. Because individual spikes can be as short as 1 ms, it has been a difficult detection problem to resolve individual events with traditional fast voltage-sensitive dyes. The temporally expanded response of FlaSh gives a significant advantage in this respect, as the area under the response is ~30-fold larger than the area under the input spike (converting units appropriately). This temporal amplification makes single spikes 30 times easier to detect than they would be with a fast dye with a comparable fractional fluorescence change.

Although the response from FlaSh extends over 100 ms, the resolution with which individual spikes can be resolved is significantly better than 100 ms. For example, by inspecting Figure 4, it is possible to estimate when spikes occurred to within a few milliseconds. Visual inspection would become more difficult in cases where the background noise is relatively large, as will be the case when recording from small cells in vivo. Significantly better resolution can be achieved in these cases by using linear filter theory to design an "inverse" FlaSh, i.e., a linear filter that reconstructs an unknown spike train given the fluorescent output generated by FlaSh. An impulse train is an adequate approximation to a train of action potentials, because voltage spikes (<10 ms) are typically much shorter than the characteristic fluorescence response from FlaSh (>100 ms). A linear filter approximation is appropriate as long as the sensor population does not saturate in the active state. A linear matched filter (Haykin, 1994) did succeed in recovering spike times to within at least 10 ms, even in the presence of significant amounts of noise (data not shown).

#### Flexible Operating Range and Targeting of Sensor

One advantage of using the Shaker channel is that many mutations have been described that produce unique alterations in its voltage dependence and kinetics. This provides flexibility in the design of optical voltage sensors with an operating range that best suits the signals of interest. For example, mutants with more negative operating range can be used to detect inhibitory and subthreshold excitatory synaptic activity, whereas mutants that operate at more positive potentials may be used to detect action potentials exclusively.

In the case of both passive dendrites or active axons, the magnitude of fluorescence change will be proportional to the excitatory activity. These two kinds of activity may be studied separately by selectively targeting FlaSh to dendrites, axons, or synapses. Heterologous proteins can be targeted to subcellular regions by genetically attaching peptide sequences that are localized by the transport machinery of the cell. This has been accomplished previously in several instances, including the synaptic localization of a membrane protein in vivo

(Mostov et al., 1992; Callahn and Thomas, 1994; Clark et al., 1994; Zito et al., 1997, submitted).

#### Conclusion

The success of the Shaker-GFP fusion protein as an optical voltage sensor suggests that the modular approach to the production of optical sensors may be expanded to the real-time detection of other signaling events. The constructs could include *GFPΔC* as a reporter, a signal transduction protein as a detector, and, if desired, a subcellular targeting peptide. The most obvious variant of this would be to insert *GFPΔC* just after S6 in cyclic nucleotide-gated channels or  $\text{Ca}^{2+}$ -gated channels, so as to make a sensor for the local, sub-membrane concentration of these second messengers. Such constructs may make possible the noninvasive detection of activity in a variety of proteins, including receptors, G proteins, enzymes, and motor proteins. The developmental timing and cellular specificity of expression can be controlled by placing the construct under the transcriptional control of a specific promoter. The combined ability to tune the sensor module via mutagenesis and to target the sensor to specific locations affords powerful advantages for the study of signal transduction events in intact tissues.

#### Experimental Procedures

##### Construction of the FlaSh Membrane Probe

We amplified *GFPΔC* from the plasmid TU#65 (Chalfie et al., 1994) using the polymerase chain reaction with primer sequences CCAC TAGTAAAGGAGAAGAAGCTTTTC and GGACTAGTGCCATGTGTAAT CCCAGCAGCTGT. These primers amplify amino acids 2–233 of GFP and add *SpeI* restriction sites in-frame to both ends. *ShH4* (gift of Ligia Toro) had been cloned into pBluescript (Stratagene), and site-directed mutagenesis was used to engineer the point mutation *W434F*, which blocks ionic current through the channel. *GFPΔC* was inserted into *ShH4-W434F* at the *SpeI* restriction site by using standard techniques, and the orientation of the insert was verified by digesting with *NcoI*, which cuts asymmetrically in *GFPΔC* and *ShH4*. We also digested with *HpaI* to verify that only a single copy of *GFPΔC* was inserted into *ShH4-W434F*. The FlaSh cDNA was transcribed using Megascript T7 (Ambion, Austin, TX) with a 4:1 methyl CAP to rGTP ratio, and the precipitated cRNA was resuspended in Ultrapure water (Specialty Media, Laballette, NJ) for injection.

##### Voltage-Clamp Fluorimetry and Analysis

Oocyte isolation, injection, and incubation were as described previously (Isacoff et al., 1990). Two-electrode voltage clamping was performed with a Dagan CA-1 amplifier (Dagan Corporation, Minneapolis, MN). External solution was NaMES (110 mM NaMES, 2 mM  $\text{Ca}[\text{MES}]_2$ , and 10 mM HEPES [pH 7.5]). Capacitance compensation was performed from a holding potential of 60 mV. An HC120-05 photomultiplier (Hamamatsu, Bridgewater, NJ) was used for fluorescence measurements, on a Nikon TMD inverted microscope. Data was sampled at 4 kHz and fluorescence signals were low-pass filtered at 1 kHz with an 8-pole Bessel filter (Frequency Devices, Haverhill, MA). Data was acquired onto a Digidata 1200 A/D interface (Axon Instruments, Foster City, CA). Data acquisition and analysis were done with Axon Instruments Pclamp 6. Illumination was with a 100 W Hg Arc lamp. Exciting and emitted light were filtered through an HQ-GFP filter (Chroma Technology, Brattleboro, VT), with the following bandpass: excitation filter, 425–475 nm; dichroic, 480 nm long-pass; emission filter, 485–535 nm.

Charge-voltage relations were constructed from the integrated off gating currents, evoked by repolarizations to –80 mV, after depolarizations that were long enough for the on gating current to decay to completion. Fluorescence-voltage relations were constructed

from the amplitudes of the "on" fluorescence change from steps long enough to reach steady state. Fluorescence traces in Figures 4A–4E were digitally RC filtered at 300 Hz. Linear reconstructions in Figures 4F and 4G were performed with Matlab software (Math-Works).

Confocal images were acquired on a Nikon PCM-2000 microscope using the 488 nm line of an Argon laser. Images were analyzed using the public domain NIH Image program (developed at the U. S. National Institutes of Health).

#### Acknowledgments

We thank Scott Fraser, Henry Lester, Carver Mead, Gilles Laurent, Norman Davidson, John Ngai, and members of the Isacoff lab for helpful discussions; Tom Alber and Shane Atwell for advice on protein engineering; Cesar Labarca for help with molecular biology during the initial stage of this project; and Joseph Dynes for assistance with the confocal microscopy. Sanjoy Mahajan gave advice on the physical limits of signal detection and suggested that a matched filter could recover the original spike train. Research supported by the McKnight and Klingenstein foundations. M. S. S. is a Howard Hughes Predoctoral Fellow in the Biological Sciences.

Received August 28, 1997; revised September 16, 1997.

#### References

- Amsterdam, A., Lin, S., and Hopkins, N. (1995). The *Aequorea victoria* green fluorescent protein can be used as a reporter in live zebrafish embryos. *Dev. Biol.* 171, 123–129.
- Baukrowitz, T., and Yellen, G. (1995). Modulation of  $K^+$  current by frequency and external  $[K^+]$ : a tale of two inactivation mechanisms. *Neuron* 15, 951–960.
- Baumann, A., Grupe, A., Ackermann, A., and Pongs, O. (1988). Structure of the voltage-dependent potassium channel is highly conserved from *Drosophila* to vertebrate central nervous system. *EMBO J.* 7, 2457–2463.
- Bezanilla, F., Perozo, E., Papazian, D.M., and Stefani, E. (1991). Molecular basis of gating charge immobilization in Shaker potassium channels. *Science* 254, 679–683.
- Callahn, C.A., and Thomas, J.B. (1994). Tau-beta-galactosidase, an axon-targeted fusion protein. *Proc. Natl. Acad. Sci. USA* 91, 5972–5976.
- Chalfie, M., Tu, Y., Euskirchen, G., Ward, W.W., and Prasher, D.C. (1994). Green fluorescent protein as a marker for gene expression. *Science* 263, 802–805.
- Christie, M.J., North, R.A., Osborne, P.B., Douglass, J., and Adelman, J.P. (1990). Heteropolymeric potassium channels expressed in *Xenopus* oocytes from cloned subunits. *Neuron* 4, 405–411.
- Clark, I., Giniger, E., Ruhola-Baker, H., Jan, L.Y., and Jan, Y.N. (1994). Transient posterior localization of a kinesin fusion protein reflects anteroposterior polarity of the *Drosophila* oocyte. *Curr. Biol.* 4, 289–300.
- Cohen, L., and Leshner, S. (1986). Optical monitoring of membrane potential: methods of multisite optical measurement. *Soc. Gen. Physiol.* 40, 71–99.
- Covarrubias, M., Wei, A., and Salkoff, L. (1991). Shaker, Shal, Shab, and Shaw express independent  $K^+$  current systems. *Neuron* 7, 763–773.
- Dopf, J., and Horiagon, T.M. (1996). Deletion mapping of the *Aequorea victoria* green fluorescent protein. *Gene* 173, 39–44.
- Drewe, J.A., Verma, S., Frech, G., and Joho, R.H. (1992). Distinct spatial and temporal expression patterns of  $K^+$  channel mRNAs from different subfamilies. *J. Neurosci.* 12, 538–548.
- Gonzalez, J.E., and Tsien, R.Y. (1997). Improved indicators of cell membrane potential that use fluorescence resonance energy transfer. *Chem. Biol.* 4, 269–277.
- Gross, D., and Loew, L.M. (1989). Fluorescent indicators of membrane potential: microspectrofluorometry and imaging. *Methods Cell Biol.* 30, 193–218.
- Haykin, S.S. (1994). *Communication Systems*, Third Edition (New York: Wiley).
- Heim, R., Prasher, D.C., and Tsien, R.Y. (1994). Wavelength mutations and posttranslational autooxidation of green fluorescent protein. *Proc. Natl. Acad. Sci. USA* 91, 12501–12504.
- Hoshi, T., Zagotta, W.N., and Aldrich, R.W. (1990). Biophysical and molecular mechanisms of Shaker potassium channel inactivation. *Science* 250, 533–538.
- Hoshi, T., Zagotta, W.N., and Aldrich, R.W. (1991). Two types of inactivation in Shaker  $K^+$  channels: effects of alterations in the carboxy-terminal region. *Neuron* 7, 547–556.
- Isacoff, E.Y., Jan, Y.N., and Jan, L.Y. (1990). Evidence for the formation of heteromultimeric potassium channels in *Xenopus* oocytes. *Nature* 345, 530–534.
- Kamb, A., Tseng-Crank, J., and Tanouye, M.A. (1988). Multiple products of the *Drosophila Shaker* gene may contribute to potassium channel diversity. *Neuron* 1, 421–430.
- Levy, D.I., and Deutsch, C. (1996). A voltage-dependent role for  $K^+$  in recovery from C-type inactivation. *Biophys. J.* 71, 3157–3166.
- Li, M., Jan, Y.N., and Jan, L.Y. (1992). Specification of subunit assembly by the hydrophilic amino-terminal domain of the Shaker potassium channel. *Science* 257, 1225–1230.
- Marshall, J., Molloy, R., Moss, G.W.J., Howe, J.R., and Hughes, T.E. (1995). The jellyfish green fluorescent protein: a new tool for studying ion channel expression and function. *Neuron* 14, 211–215.
- McCormack, K., Lin, J.W., Iverson, L.E., and Rudy, B. (1990). Shaker  $K^+$  channel subunits form heteromultimeric channels with novel functional properties. *Biochem. Biophys. Res. Comm.* 171, 1361–1371.
- Mostov, K., Apodaca, G., Aroeti, B., and Okamoto, C. (1992). Plasma membrane protein sorting in polarized epithelial cells. *J. Cell Biol.* 116, 577–583.
- Nobile, M., Olcese, R., Toro, L., and Stefani, E. (1997). Fast inactivation of Shaker  $K^+$  channels is highly temperature dependent. *Exp. Brain Res.* 114, 138–142.
- Ormo, M., Cubitt, A.B., Kallio, K., Gross, L.A., Tsien, R.Y., and Remington, S.J. (1996). Crystal structure of the *Aequorea victoria* green fluorescent protein. *Science* 273, 1392–1395.
- Perozo, E., MacKinnon, R., Bezanilla, F., and Stefani, E. (1993). Gating currents from a nonconducting mutant reveal open-closed conformations in Shaker  $K^+$  channels. *Neuron* 11, 353–358.
- Prasher, D.C., Eckenrode, V.K., Ward, W.W., Prendergast, F.G., and Cormier, M.J. (1992). Primary structure of the *Aequorea victoria* green-fluorescent protein. *Gene* 111, 229–233.
- Ruppersberg, J.P., Schroter, K.H., Sakmann, B., Stocker, M., Sewing, S., and Pongs, O. (1990). Heteromultimeric channels formed by rat brain potassium-channel proteins. *Nature* 345, 535–537.
- Shen, N.V., Chen, X., Boyer, M.M., and Pfaffinger, P.J. (1993). Deletion analysis of  $K^+$  channel assembly. *Neuron* 11, 67–76.
- Stuhmer, W., Ruppersberg, J.P., Schroter, K.H., Sakmann, B., Stocker, M., Giese, K.P., Perschke, P., Baumann, A., and Pongs, O. (1989). Molecular basis of functional diversity of voltage-gated potassium channels in mammalian brain. *EMBO J.* 8, 3235–3244.
- Tempel, B.L., Papazian, D.M., Schwarz, T.L., Jan, Y.N., and Jan, L.Y. (1987). Sequence of a probable potassium channel component encoded at Shaker locus of *Drosophila*. *Science* 237, 770–775.
- Timpe, L.C., Jan, Y.N., and Jan, L.Y. (1988). Four cDNA clones from the Shaker locus of *Drosophila* induce kinetically distinct A-type potassium currents in *Xenopus* oocytes. *Neuron* 1, 659–667.
- Tsien, R.Y. (1989). Fluorescent probes of cell signaling. *Annu. Rev. Neurosci.* 12, 227–253.
- Ward, W.H., Prentice, H.J., Roth, A.F., Cody, C.W., and Reeves, S.C. (1982). Spectral perturbations of the *Aequorea* green-fluorescent protein. *Photochem. Photobiol.* 35, 803–808.
- Yang, F., Moss, L.G., and Phillips, G.N. (1996). The molecular structure of green fluorescent protein. *Nat. Biotechnol.* 14, 1246–1251.
- Zagotta, W.N., Hoshi, T., and Aldrich, R.W. (1990). Restoration of inactivation in mutants of Shaker potassium channels by a peptide derived from ShB. *Science* 250, 568–571.